Received Date: Sept. 2024 Revised: Nov. 2024 Accepted: Dec. 2024

Investigation of Organic Fraction of Mahonia Nepalensis for Effective Corrosion Prevention of Mild Steel

Anju Kumari Das[1,2], Maya Das[1], Nabin Karki [3], Dipak Kumar Gupta [1#] and Amar Prasad Yadav[1#a]

[1]*Central Department of Chemistry, Tribhuvan University, Kirtipur, Kathmandu, Nepal*

[2]*Amrit Science Campus, Tribhuvan University, Kathmandu, Nepal*

[3]*Bhaktapur Multiple Campus, Tribhuvan University, 44800 Bhaktapur, Nepal*

[# a] *Currently @Rajarshi Janak University (RJU), Janakpur, Nepal*

[#] ***Corresponding E-mail:*** **deepakguptas2012@yahoo.com** ***and*** **amar2y@yahoo.com**

Doi: https://doi.org/10.3126/pragya.v13i2.78778

Abstract

Plant extracts are a conceivably better substitute for corrosion prevention of metallic materials that are acceptable to the environment. This study investigates about the application of the organic fraction of Mahonia nepalensis (MN) bark extract for the corrosion protection of mild steel (MS) in 1 M H2SO4. The separation of the organic layer from MN bark extracts were subjected to column chromatography using the dichloromethane (DCM)-methanol as solvent for the separation of alkaloids. The identification and quantification of compounds of the DCM-methanol fraction was performed by liquid column mass spectrometry (LC-MS). Fourier transform infrared (FTIR) and ultraviolet-visible spectroscopy (UV-Vis) were used to characterize the DCM-methanol fraction of the MN extract. Potentiodynamic polarization (PDP) and electrochemical impedance spectroscopy (EIS) were used to investigate the corrosion inhibition of MS using the DCM-Methanol fractions in 1M H_2SO_4. The DCM-Methanol fraction containing 1.2 ppm berberine exhibited an inhibitory efficiency (IE) of 84.35%, suggesting that it is a viable and reasonable choice for preventing MS corrosion. The potentiodynamic polarization reflected a decrease in the hydrogen reduction, as indicated by the suppression of the cathodic current without altering the reaction process. According to open circuit potential and polarization curves, it showed mixed inhibitory behavior. EIS analysis also found a decrease in double-layer capacitance and an increase in charge transfer resistance. EIS and energy dispersive X-ray spectroscopy (EDX) in a scanning electron microscope (SEM) confirmed inhibitor molecules have adhered to the MS surface to form a protective coating.

Keywords: Berberine, Dichloromethane - Methanol Fraction, LCMS, EIS, and Green Corrosion Inhibitor

1. Introduction

Mild Steel (MS) is widely used as a structural material because of its affordability and great mechanical strength (Gupta *et al*., 2021). It is an important convenience including pipelines, and bridges due to its low-cost replacement, maintenance and loss of productivity. The

application of paint coats has proven beneficial in establishing a barrier of protection. One crucial component of paints is using pigments that prevent corrosion (Díaz et al., 2012; Hooshmand Zaferani et al., 2013; B. Li et al., 2023; Oyekunle et al., 2019). Because of its high sensitivity to environmental factors through chemical and electrochemical processes, corrosion causes damage to component metals. Surface damage leads to corrosion, which results in cross section damage causing decreased ductility and strength. It also leads to structural failure and machine shutdown (Habeeb et al., 2018). The majority of corrosion issues worldwide are caused by environmental and facility factors. Although corrosion may not directly harm a material, it can have an impact on its strength, mechanical behavior, and appearance, which can lead to significant working problems (B. Li et al., 2023). Acidic pickling, acidizing, de-scaling, and chemical cleaning are the primary uses of acidic solutions in industry. Sulphuric acid (H_2SO_4) and hydrochloric acid (HCl) are the most frequently utilized. Naturally, corrosive environments are the cause of these, which leads to severe corrosion issues in industrial operations. Acid corrosion inhibitors are used extensively to reduce or stop acid-related material loss (Peter & Sharma, 2017).

An estimated US$2.5 trillion, or 3.4% of global GDP, is currently lost owing to corrosion globally. It is predicted that 15% to 35% of the cost of corrosion might be reduced by employing suitable corrosion management measures. Traditionally, these expenses do not account for particular environmental or safety implications. Many industries have realized that improper corrosion management may be quite expensive and that, throughout an asset's lifespan, substantial expenses can be diminished by effective corrosion management (Koch, 2017). In Industry equipment that has been exposed to corrosion can be cleaned with sulphuric and hydrochloric acids, which are used in a variety of ways to remove rust from metal surfaces. In this process, a corrosion protection method should be used to prevent metal from corroding. In recent years, one of the existing and promising methods to reduce the pace and effects of corrosion is the use of inhibitors. Several variables (material type, acidic or basic conditions) affect the corrosion rate and its mechanism. In a corrosive environment, Mild Steel (MS) surface degradation occurs according to the following reaction:

$$M+2H^{+} \longrightarrow M^{2+}+H_2$$

Ions are transferred from the anode or cathode side in this process. MS undergoes an electrochemical reaction that comprises oxidation and reduction processes.

At the anode, metal dissolution occurs:

$$M \longrightarrow M^{2+}+2e^-$$

At the cathode, the reduction of hydrogen ions occurs:

$2H^+ + 2e- \rightarrow H_2$

Hydrogen gas is evolved as the product of corrosion (Ahmed & Zhang, 2019; El Hamdani et al., 2015; Habeeb et al., 2018; Krishnegowda et al., 2013)

Inhibitors are compounds (or a mixture of substances) used in extremely small quantities to treat the metal surface exposed to a corrosive atmosphere. This reduces or stops the metal from corroding. Because of their adsorptive qualities, they are sometimes referred to as adsorption site blockers, blocking species, or site-blocking components. Naturally biocompatible materials are called "green inhibitors" or "eco-friendly inhibitors." The biological nature of the inhibitors, such as plant extracts, suggests that they are biocompatible (Singh, 2013).

Numerous synthetic inhibitors contain toxic or harmful chemicals that can fatal the environment. Their removal can lead to pollution making them unsuitable for environmentally sensitive applications. Numerous countries have strict regulations on the use of synthetic chemicals due to health, safety, and environmental concerns. This limits the use of certain synthetic inhibitors. Due to these limitations, industries often explore alternative corrosion control methods such as green inhibitors (derived from plant extracts), coating (e.g., Polymeric or ceramic coatings), cathodic protection, and material selection (using inherently corrosion-resistant alloys).

The adsorption of inhibitor molecules on metal surfaces is facilitated by their pi electron in molecule structure. This structure is influenced by the substance, surface charge, corrosive medium type, and metal molecular structure. Uses for some corrosion inhibitors vary depending on the climate and significantly reduce the metal's ability to dissolve. By slowing down metal dissolution, hydrogen ion reduction, or both, inhibitor adsorption can alter the double-layer structural properties in acid corrosion (Das et al., 2024).

Several investigations have demonstrated that plant extracts, such as those from *Glycyrrhiza glabra* leave (Alibakhshi et al., 2018) *Rosa canina* fruit (Sanaei et al., 2019), *Azadirachta indica* (AZI), *Cassia senna* (Karthik et al., 2014), *Equistetum hyemale* (Karki, et al., 2021), *Berberis Aristrata* (Karki et al., 2020), etc are efficient green inhibitors. Since 1970, several investigations on alkaloids for corrosion inhibition have been performed, primarily in sulphuric acid and hydrochloric acid. Crude plant extracts have been reported as green corrosion inhibitors. Very few investigations on the separation and isolation of alkaloid molecules have been reported for the effective inhibition of metal corrosion. Berberine is among the alkaloids that have been investigated to prevent MS corrosion in acidic environments. Similarly, quinine, piperine, vasicinone, isopelletierine, multiflorine, and

indole have also been studied as corrosion inhibitors (Karki, et al., 2021; Kaya et al., 2023; Das et al., 2024).

In Nepal, many plant-based extracts have been studied and applied as eco-friendly corrosion inhibitors due to bioactive compounds such as alkaloids, flavonoids tannins, and essential oils. Some of the commonly used plants for this purpose include *Azadirachta indica* (Neem), *Curcuma longa* (Tumeric), *Psidium guajava* (Guava), *Euphorbia royleana*, *Moringa oleifera* (Moringa), *Aloe barbadensis* (Aloe vera), *Lantana camara, Euphorbia pulcherrima* etc(Gupta et al., 2020; Das et al., 2024). Research institutions and industries in Nepal are increasingly exploring these plants to develop sustainable corrosion prevention methods.

This research investigates about the usefulness of corrosion inhibition of separated alkaloids from MN extract onto mild steel in an acid solution. The dichloromethane (DCM) methanol solvent was used in different proportions to separate alkaloids from the MN extract by column chromatography. The fractions M21 and M26 are found to contain berberine (the structure of the molecule is displayed in Fig. 1). Liquid Column Mass Spectroscopy (LCMS) was used to confirm and quantify berberine. Both fractions containing berberine at a concentration of around 1 ppm are enough and effective in preventing MS corrosion. In the presence of an inhibitor solution, the MS dissolution slowed down in an acidic solution, and, the stabilized open circuit potential (OCP) formed a potential thin film over the MS surface immediately. The goal was to investigate the corrosion inhibition properties using the electrochemical polarization technique and the adsorption kinetics and process by electrochemical impedance spectroscopy (EIS).

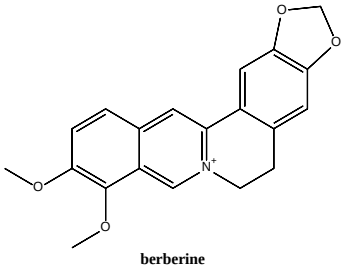

Fig. 1: Structure of Berberine

Berberine, a natural isoquinoline alkaloid, has been studied for its corrosion inhibition properties on metals such as mild steel and aluminum in acidic environments. It forms an adsorbed protective layer on the metal surface, reducing electrochemical reactions. jatrorrhizines (structurally similar to berberine) have been studied for their inhibition behaviour.

Alkaloids like quinine, nicotine, strychnine, and papaverine have been tested on mild steel, copper, and aluminum, showing inhibition through nitrogen and oxygen donor atoms. Berberine is naturally derived, and it aligns with sustainable corrosion inhibition strategies. It focuses on extracting these alkaloids from *Mahonia nepalensis* and other plant sources for large-scale applications(Y. Li et al., 2005; Parajuli et al., 2022).

The study separates organic and aqueous layers, followed by fractionation using a DCM-methanol system.LC-MS analysis confirms the presence of berberine in different fractions, demonstrating an efficient extraction strategy. This highlights the potential of berberine-rich organic extracts as effective green corrosion inhibitors. Unlike traditional studies that focus solely on crude extracts, this research investigates organic fractions, broadening the scope of corrosion inhibition mechanisms. The correlation between berberine concentration and inhibition efficiency establishes a direct structure-activity relationship. This study provides new insights into *Mahonia Nepalensis* (MN) as a promising plant-based source of alkaloids for corrosion protection, contributing to sustainable and eco-friendly inhibitor development.

2. Materials and Methods

Mahonia Nepalensis (MN) bark was collected from Godawari, Lalitpur (Latitude: 27◦60′15.63″ Longitude: 85◦36′52.96″). The bark was then chopped into small pieces and allowed to dry for a month in the shade. Using the grinding machine, it was ground into a powder, and the power was fascinated with hexane for a full day to de-fractionate and remove the green color. After that, it was filtered. The residue was then subjected to cold percolation with methanol for 7 days and filtered. Tartaric acid (>99% Merk Germany) having pH 5(3%) was added to the filtrate for acidification it and then base NH_4OH (28% Merk Germany) was added to bring the pH to 10. The methanolic extract was obtained using dichloromethane (DCM) by separating funnel. The organic layer was separated and taken in a rotator evaporator. It was evaporated at 60 ^{o}C and the process was repeated thrice to get the high yield. The concentrated extract was further evaporated in a water bath setting at 35˚C until it dried. Hence, dry alkaloids were separated.

2.1 Column Chromatography of Organic Fraction for the Separation of Alkaloids

1g of *Mahonia nepalensis* organic layer extract was dissolved in 40 mL of methanol (Fisher Scientific, UK). A column (60 cm long with 3 cm diameter) was filled with 20.07g of silica gel (60-120) slurry. The column was first eluted using a hexane gradient. The solvent media DCM (Merk, Germany) and methanol in various ratios were used to separate the alkaloids. The fractions M21 and M26 were collected using 17 mL DCM and 3 mL methanol and 14

mL DCM and 6 mL methanol respectively. The fractions were characterized by Ultra violet-visible spectroscopy (UV-Vis) and Fourier Transform Infrared (FTIR). The alkaloids were Identified and quantified by Liquid column mass spectroscopy **(**LC-MS). The electrochemical tests were carried out for the solution fractions prepared in 1 M H_2SO_4 (98% Merk Germany)

2.2 Mild Steel Sample

The steel is an alloy of iron and carbon. However, many steels contain almost no carbon. Carbon contents of some steels are as low as 0.002% by weight. The most commonly used steels are low-carbon steels. The carbon content of steel is less than 0.06% in carbon. The composition of the MS was carbon (0.17%), silicon (0.40%), manganese (0.8%), Sulphur (0.04%), phosphorous (0.04%), and iron (98.48%) (Hosford, 2012).

The mild steel (MS) samples were prepared by cutting into the desired size (3 cm × 3 cm × 0.16 cm) after being gathered from the Kathmandu local market. The polished samples were washed and sonicated with hexane. After polishing with silicon carbide paper of several gride sizes (1200, 1500, 1800, and 2000), each of the samples was then sonicated in ethanol for 20 minutes and dried. After sonication, all samples were stored in a desiccator for further use.

2.3 Characterization of Organic Fraction

*Fourier Transform Infrared (FTIR***) Spectroscopy**

To identify the presence of functional groups, Fourier Transform Infrared (FTIR) Spectroscopy (PerkinElmer10.6.2 spectrum) was used. Organic fraction (M21 and M26) of MN extract dissolved in methanol was used to perform FTIR characterization within the wavelength of 500 to 4000 cm^{-1} (Hossain et al., 2022).

Ultra-Visible spectroscopy

A double-beam UV-visible spectrophotometer (Labtronics 2802) was used to record the UV-visible spectra of the organic fraction (M21 and M26) of the MN extract in methanol. Each sample was taken in a 2.0 mL quartz cuvette with a 1.0 cm path length and scanned from 200 to 800 nm wavelength. Fractions were diluted ten times with methanol by Lambert-Beer's law. Methanol was taken as the blank, and absorption was adjusted to zero.

2.4 Liquid column mass spectroscopy (LC-MS)

Separated compounds in various fractions of DCM-Methanol were analyzed and quantified using a Shimadzu Prominence HPLC (LC 20 AD) equipped with a single quadrupole mass detector (LCMS 2020). SIM and SCAN were the modes of acquisition. Data processing was done using Shimadzu LC-MS LabSolutions version 5.98 SP1 (Shimadzu Corp., Japan). The chromatographic separation was performed using an ACE C18 column (100×2.1 mm, 1.8 μm, Advanced Chromatography Technologies, USA). 0.5 μL volume of each fraction was injected. The solvent mixture of 0.1% formic acid and methanol was applied to elute berberine. The flow rate was set as 0.2 mL min^{-1} for the elution of each sample and the temperature was set at 40 °C. Following the first 3.8 minutes of each run, the elution from the LC column was routed from the trash to the mass spectrometer source. The ESI source was adjusted as nebulizing gas flow (3 L min^{-1}), 250 °C for the dissolution line temperature, drying gas flow (11 L min^{-1}), and 350 ◦C for the heat block temperature. In SIM mode, the sample was observed for a mass per charge (m/z) value of 336 (Hua wenyan et al., 2007).

2.5 Surface characterization by Scanning electron microscope (SEM) and Energy Dispersive X-ray (EDX) analysis

A scanning electron microscopy (SEM) Port JSM-300 electron microscope was employed to examine the adsorption of separated compounds on the surface of Mild Steel (MS). The elemental composition was examined by Energy-dispersive X-ray Analysis (EDX). The investigation was performed using a Port JSM-300 electron microscope (CSIR-IMMT, India)

2.6 Corrosion test by electrochemical measurements

Potentiodynamic polarization

A glass cell with three electrodes was used to perform electrochemical studies. A saturated calomel electrode (SCE) was employed as the reference electrode. A platinum electrode was employed as the counter electrode, and an MS sample with a 0.608 cm^2 exposed surface area was used as the working electrode. For the electrochemical measurements, the open circuit potential (OPC) of MS was recorded for 30 minutes. The potentiodynamic polarization (PDP) was scanned from OCP to ± 300 mV at a rate of 1 mV/s. Echem Analyst software was used to determine the cathodic and anodic slopes from the polarization curves. The Gamry framework software and a Gamry potentiostat (Reference 600) were used to calculate the corrosion potential (Ecorr), corrosion current density (color), and corrosion inhibition efficiency (IE). All measurements were performed at Room Temperature (RT).

The room temperature was 25^0C (298K). Using relation (1), the Inhibition Efficiency (IE%) was determined.

$$IE\% = \frac{i^0_{corr} - i_{corr}}{i^0_{corr}} \times 100 \qquad (1)$$

$_{your}$ and i^0_{corr} are current densities with and without inhibitor solution respectively (Hussin et al., 2016)

Electrochemical impedance spectroscopy (EIS)

Gamry Instrument was used to perform Electrochemical Impedance Spectroscopy (EIS) with a 1 mV s^{-1} scan rate within 100 kHz to 0.01 Hz frequency range at room temperature i.e., 25^0C(298K). ZView software was used to evaluate the experimental data. The relation (2) was applied to determine the inhibition efficiency IE.

$$IE(\eta)\% = \frac{R_{p-R^0_P}}{R_p} \times 100 \qquad (2)$$

R_p and R_p^0 are the polarization resistance resistances without and with inhibitors respectively.

3. Results and Discussion

3.1 UV–visible spectra

Fig. 2 displays the UV-vis spectra of the M26 fraction of MN extract. The absorption spectra show absorption peaks at 235nm and 310 nm. The peak 235nm is near the UV region. This peak corresponds to $\pi \rightarrow \pi^*$electronic transitions in conjugated double bond or aromatic rings. It is often associated with unsaturated systems or conjugated dienes in the alkaloid structure. In MN berberine and jatrorrhizine contain isoquinoline structures, which contribute to strong absorption in this region. It indicates chromophoric groups such as methylenedioxy (-O-CH_2-O) and phenolic rings which absorb UV light around this range. The peak at 310nm shows a far UV region. The longer wavelength absorption is indicative of $n \rightarrow \pi^*$ often occurs in functional groups with pairs such as C=O or amines.

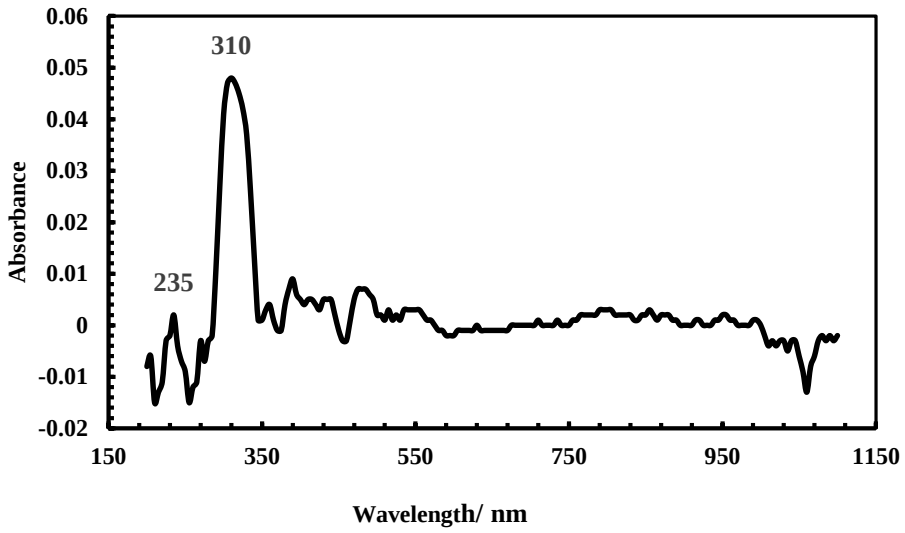

Fig. 2: UV visible spectra of M26 fraction of MN extract

3.2 Fourier Transform Infrared (FTIR) spectra of Organic fraction

Fig. 3 represents ATR-FTIR spectra of the organic fraction of *Mahonia Nepalensis* with representative functional groups.

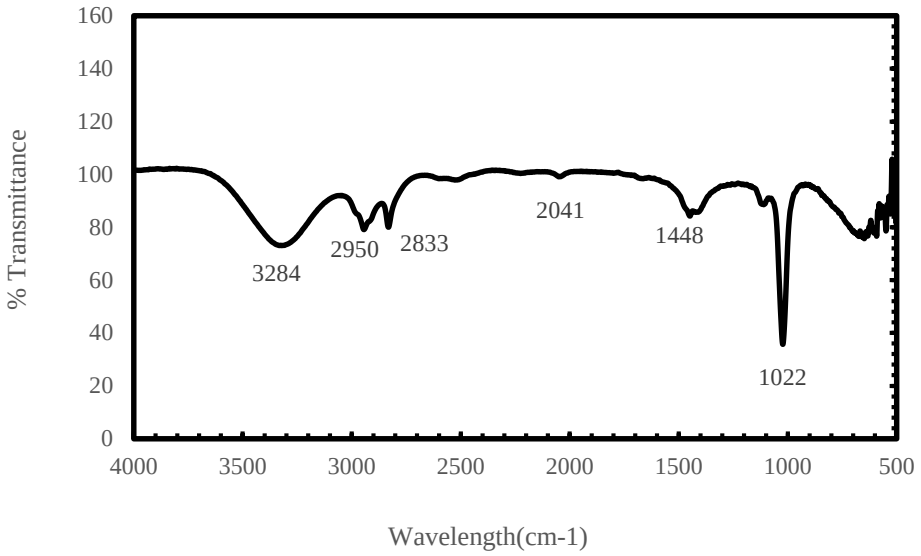

Fig. 3:

FTIR of M26 fractions of MN extract

The peaks are located in a wide range of spectra. The peak at 3284cm^{-1},2950cm^{-1},1448cm^{-1}, 1022 cm^{-1} shows O-H stretching N-H stretching, C-H bending and C-O stretching. The extract's main constituents include nitrogen, oxygen atoms, and aromatic rings, according to the FTIR analysis's findings. Similar FTIR bands have been found in MN phytochemical investigations (Kaya et al., 2023)

3.3 Liquid Column Mass Spectroscopy (LC-MS)

LC-MS data represented the presence of Berberine having m/z value of 336 and matched with the standard berberine's mass ([M H] + (m/z 336.1247), **Fig. 4** shows chromatogram **and Fig. 5** reflects the identities, retention times, and detected molecular and protonated ion of berberine.

The two different fractions of MN have different concentration of berberine with different retention time as shown in Table 1. In case of M21 and M26 fraction the concentration of berberine was found to be 0.922 and 1.146 ppm respectively.

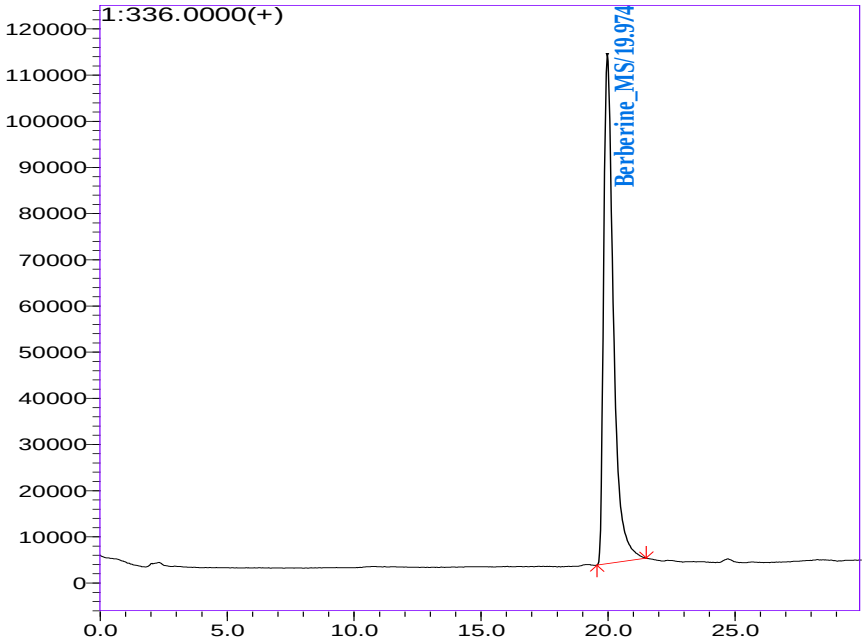

Fig. 4: Extracted ion chromatogram of sample number M26 $[M+H]^+$=336

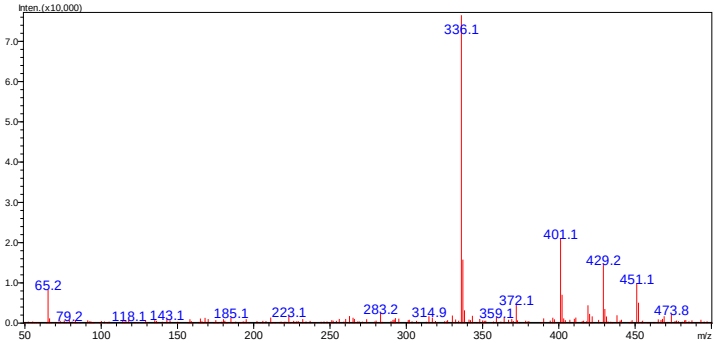

Fig .5: Mass spectra of berberine

Table 1: Concentration of berberine in different organic fractions along with retention periods and molecular mass

Fraction	Ret Time	m/z	Concentration of berberine (ppm)
M21	19.992	336.1	0.922
M26	20.017	336.1	1.146

3.4 Open circuit potential (OCP) of Organic Fractions

The OCP of the MS in the presence of an inhibitor provides information about the inhibitor's corrosion control mechanisms and the potential surface charge. **Fig. 6** represents the OCP of the MS sample in M21 and M26 fractions in 1 M H_2SO_4 and 1 M H_2SO_4.

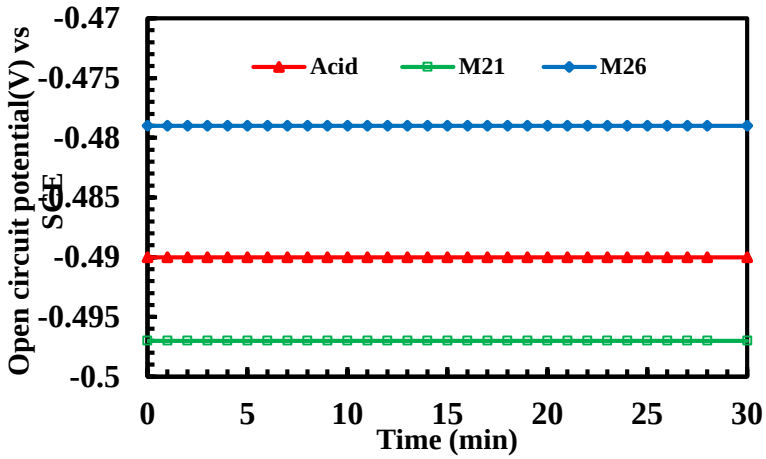

Fig..6: Open circuit potential with time in 1 M H_2SO_4, M21, and M26 at room temperature

The OCP of MS in the acid solution was - 0.490 V and remained constant for 30 min. The OCP of M21 was - 0.497V which also remained constant for 30 min but the OCP of M21

fraction is slightly negative than acid. In the case of the M26 fraction, the OCP is -0.479 mV which is more positive than the OCP of acid suggesting the formation of a passive layer on the metal surface by inhibitor molecules. This can reduce the anodic reactions (metal dissolution). The change in OCP of MS in inhibitor solution is marginal (less than 85mv) showing the inhibitory property is of mixed type (Karki, et al., 2021).

3.5 Potentiodynamic Polarization (PDP)

The polarization curves for MS in acid solution, M21 and M26 fractions are shown in **Fig.7**. The inhibition efficiency (IE%), corrosion potential (Ecorr), corrosion current density (icorr), anodic and cathodic Tafel slopes (βa and βc) are displayed in the table 3. Gradient lines were extrapolated from the experimental Tafel plots' cathodic and anodic overpotentials using Gamry Echem Software version 5.50. The current density of the MS sample is reduced in both cases M21 and M26, as seen in **Fig 7**. In presence of inhibitor, the cathodic curve sharply drops, indicating that inhibitor molecules have been absorbed and that the hydrogen reduction reaction has been retarded down. Additionally, it is seen that the cathodic curves continue to run parallel to the addition of the inhibitor, showing that the hydrogen evolution mechanism is unaffected. The reduction in anodic slope indicates inhibitor molecule desorption and, thus, increased metal dissolution. The obtained data show that inhibitors have a considerable ability to adsorb on the metal surface. Consequently, the rate of iron dissolution is reduced. The fractions M21 and M26 displayed 72% and 95% inhibition efficiency respectively (Cang et al., 2013; Wang et al., 2019).

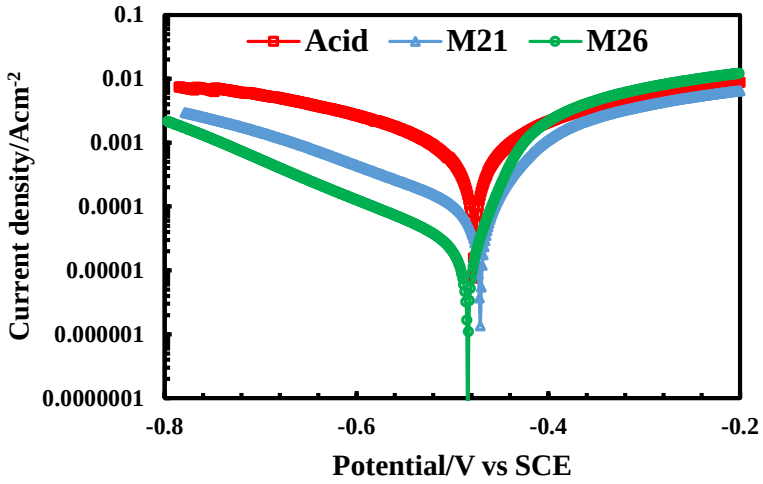

Fig. 7: Potentiodynamic polarization of MS in acid, M21, and M26 fractions at room temperature with 1 mV/s scan rate

Table 2: Potentiodynamic polarization parameters of MS in M21 and M26 organic fractions

Sample	βa(V/decade)	βc(V/decade)	Score(μA/cm2	E_{corr}(mV)	Efficiency%
Acid	0.029	- 0.066	1.70E-04	0.471	
M_{21}	0.026	- 0.026	4. 61E-5	0.468	72.88
M_{26}	0.045	- 0.05	3.61E-10	0.480	95.6

3.6 Electrochemical impedance spectroscopy (EIS)

Fig. 8 shows the Nyquist and Bode plots of the impedance data obtained for MS in M21 and M23 organic fractions. The electrode/electrolyte interface and corrosion processes taking place on mild steel surfaces in the presence of organic fractions containing different concentrations of berberine were investigated. **Fig.8 (a)** clearly shows that the diameter of the semicircle increases with increasing concentration of berberine in organic fraction, indicating an improvement in the metal's resistance to corrosion.

The ohmic resistance is given by the solution resistance (R_s), and the inhibitor's resistance to metal surface oxidation is indicated by the charge transfer resistance (R_{ct}), which is inversely correlated with the corrosion rate. As the Nyquist plot diameter increases, the R_{ct} value rises as well, indicating the increased inhibitory efficiency. As the resistance value (R_{ct}) increases, the electrical current (I) flows and therefore the number of electrons transmitted over the metal surface decreases. The ohmic law, in which V = IR, is the foundation for this. This indicates the oxidation of the metal becomes slower down. The metal surface's inhomogeneity led to reduced values of n (0.5n 1; depressed semicircle capacitive loop). The high-frequency capacitive loop is generated by the charge transfer resistance (R_{ct}). The inductive loop's connection is assigned to the adsorbed molecules. The capacitive loop's diameter, which is correlated with R_p, indicates both an enhancement in the protecting characters of the surface film and an increase in the number of inhibitor molecules adsorbed.

The impedance data given in Table 3 reveals that the values of both R_{ct} and IE% are found to increase in both M21 and M26 organic fraction, whereas the values of C_{dl} are found to decrease. This result is due to a decrease in the dielectric constant and/or an increase in the electric double layer's depth, indicating the resistance of inhibitor molecules over the mild steel/acid interface through an adsorption mechanism (Karthik et al., 2014).

Fig. 8 d shows the electrical equivalent circuit model that is best fitted to the EIS data. Rs stands for solution resistance in this circuit. RL stands for the inductive loop's resistance, and CPE is a constant phase element. The degree of non-ideality and surface heterogeneity

are established by the phase shift (n). For the surface heterogeneity caused by inhibitor adsorption and the formation of a porous layer on the electrode surface, the CPE was used in place of the Cdl in the fitting analysis (Kaya et al., 2023a). When comparing inhibitor-containing solutions to acid solutions, the effect of inhibitor concentration on the impedance characteristics revealed significant differences.

Bode analysis of phase angle was also performed to ascertain the profiles, as shown in Fig. (c). It is clear from Fig. (b) that the impedance is limited to polarization resistance when the frequency reaches a low value. These results imply that different concentration of inhibitor reveals identical adsorption mechanisms. Each Nyquist plot exhibits a little dip where the semicircle centers are below the x-axis as shown in Fig. 8 (a).

(a)

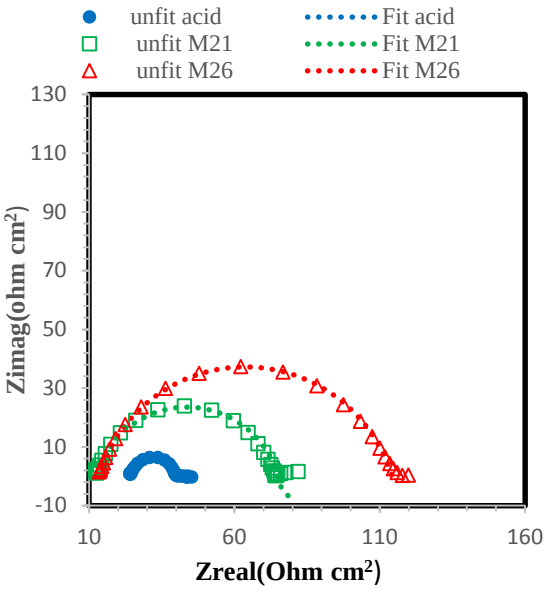

(b)

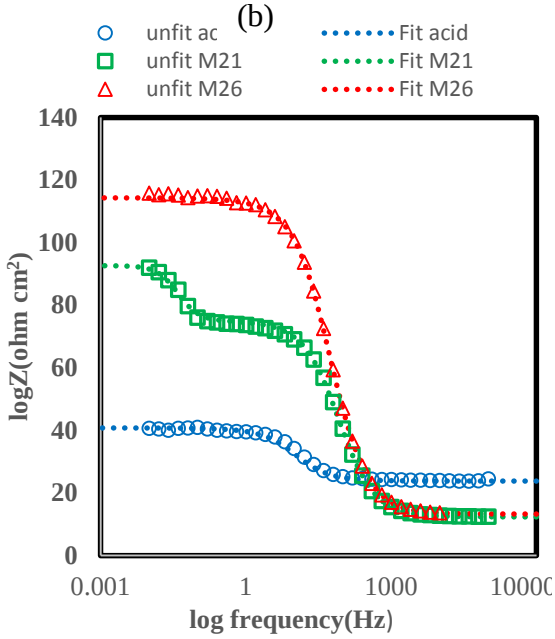

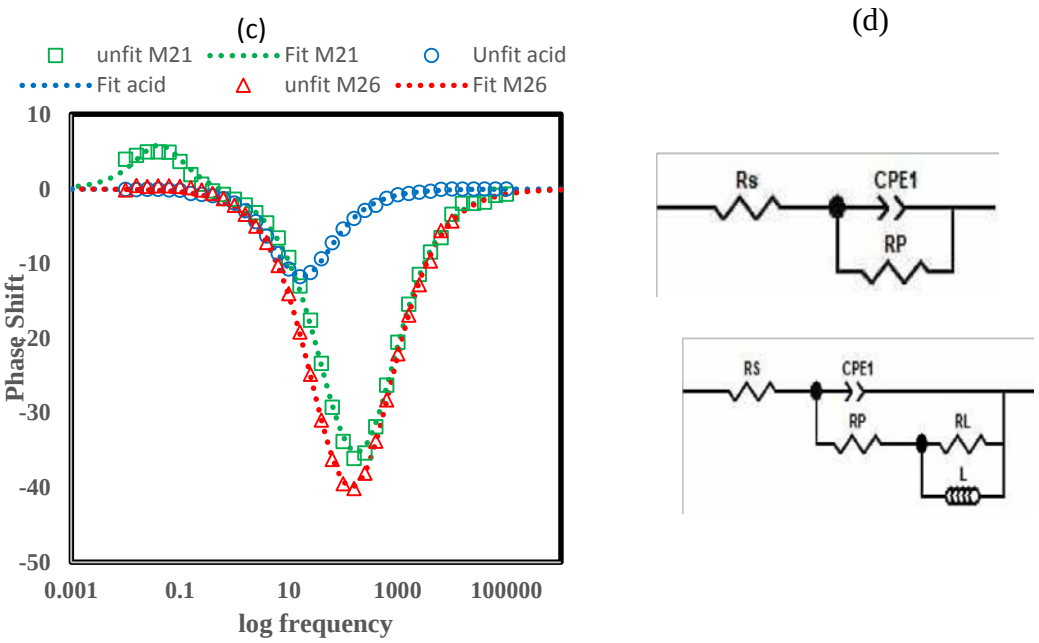

Fig. 8: (a) Nyquist plot for mild steel in 1.0M H_2SO_4, M21, and M26 fractions (b) Bode plot for mild steel in 1.0M H_2SO_4, M21, and M26 fractions (c) Bode plots of phase angle versus frequency for mild steel in 1.0 M H_2SO_4, M21, and M26 fractions (d) the equivalent circuit model to fit the impedance spectra

Table 3: Electrochemical impedance data of MS in 1.0 M H_2SO_4, with M21 and M26 fractions.

Sample	CPE (10^{-5} /s ^{n} Ω^{-1} cm^{-2})	N	R_p (Ω cm^2)	L (H)	R_L (Ω cm^2)	η %
Acid	133.82	0.8749	15.8			
M21	12.546	0.81907	80.3	75.59	-17.55	80.32
M26	11.839	0.80977	101	-53189	0.04752	84.35

3.7 SURFACE EXAMINATION STUDIES

Scanning electron microscopy (SEM) was applied to investigate mild steel (MS) surface in 1 M H2S04, M21, and M26 organic fractions as shown in **Fig. 9**. SEM micrograph reveals that MS is rough and heavily scraped due to the strong attack of acid. The **Fig. 9 (b) and**

(c) establish how the inhibitor generates a protective barrier around the mild steel surface, preventing additional acid medium attack and preventing corrosion (Hachelef et al., 2016). The energy dispersive X-ray (EDX) analysis revealed the presence C, N, O, and Fe elements on MS samples dipped in the organic fractions M21 and M26 in 1.0 M H_2SO_4. This result confirmed the formation of a shielding molecular layer caused by the adsorption of an inhibitor.

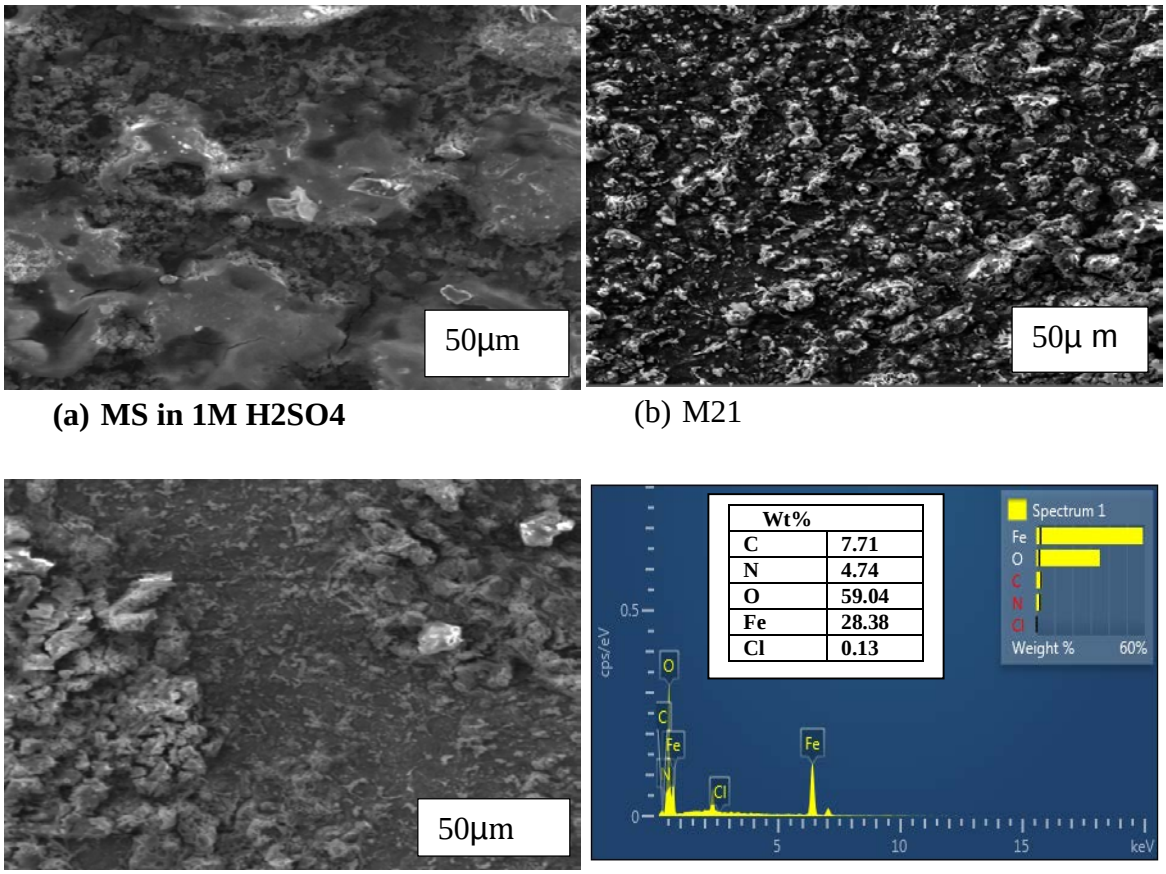

(a) MS in 1M H2SO4 (b) M21

(c)M26 (d)

Fig. 9: SEM images and corresponding EDX spectra of MS sample and isolated M21 and M26

4. Mechanism of inhibition

The types of adsorptions can be differentiated as physical adsorption mechanism or chemical adsorption mechanism or mixed type mechanism depending on interactions between metallic surface and heteroatoms and/or p-electrons of the inhibitor molecules. The

chemical structure, charge distribution, and the metal surface charge are the parameters related to the adsorption of inhibitors. In the physical adsorption mechanism, the electrically charge metal surface binds with the charge of organic inhibitors molecule. The chemical adsorption is due to the interaction of unshared free electrons of inhibitors with unoccupied d orbitals of metals forming coordinate bonds. The inhibitor molecules get adsorbed on the corroded surface of a metal. During adsorption, it removes the water molecules absorbed on the metal surface (El-Etre et al., 2005; Kadhim A et al., 2021; Okafor et al., 2012).

$$Org(sol) + aH_2O(ads) \longrightarrow Org(ads) + aH_2O(sol) \quad (3)$$

Moreover, the adsorption of organic inhibitor molecules on the metallic surface depends on the active sites, electron densities in inhibitor molecules, aromatic rings, potential steric hindrance, and the nature of the interaction between a p-orbital and iron atoms d-orbital. The adsorption of organic molecules on the metal surface can be explained on the basics of adsorption isotherms such as Langmuir (Equation 4) and Temkin (Equation 5) could explain the anti-corrosion mechanism.

$$\text{Langmuir isotherm} \quad \frac{C}{\theta} = \frac{1}{Kads} + C \quad (4)$$

$$\text{Temkin adsorption} \quad \theta = \frac{1}{f} \ln K_{ads} C \quad (5)$$

where C is the concentration of the inhibitor, K_{ads} is a constant, θ is the surface coverage degree, f is the energetic parameter, and a is the water molecules on the surface of metal. The adsorption of organic molecules on the metal surface is also affected by the structure of inhibitor molecules, charge density on the metal surface, and zero charge potency of the metal.

5. Conclusion

The berberine-containing organic fraction (DCM-Methanol) of MN bark extracts in 1 M H2SO4 exhibits an efficient corrosion inhibitor for MS. The inhibitory efficacy of the organic fractions containing about 1 ppm of berberine, was found above 80%, suggesting that it is an economical and effective alkaloid for industrial use. The polarization and open circuit potential (OCP) study showed that the separated fraction containing berberine acted as a mixed-type inhibitor controlling both anodic and cathodic processes. Electrochemical impedance spectra showed a formation of a protective layer on the mild steel surface indicated by an increase in polarization resistance (Rp) and a decrease in double-layer capacitance (Cdl). Scanning electron microscopy (SEM) with energy-dispersive X-ray (EDX) analysis exhibited the formation of protective film due to the adsorption of inhibitor molecules.

Acknowledgment

A.K Das is thankful to the University Grants Commission, Sanothimi, Nepal for providing partial financial support to this work (UGC Award No PhD-75/76S&T-3). CSIR -Central Electrochemical Research Institute, Karaikudi, Tamil Nādu, India is also acknowledged for providing SEM-EDX analysis. The authors express sincere gratitude to the National Food & Feed Reference Laboratory (NFFRL), Department of Food Technology and Quality Control (DFTC), Kathmandu, Nepal for providing the LC-MS analysis.

References

Ahmed, R. K., & Zhang, S. (2019). Alchemilla Vulgaris Extract as Green Inhibitor of Copper Corrosion in Hydrochloric Acid. *International Journal of Electrochemical Science*, *14*(11), Article 11. https://doi.org/10.20964/2019.11.43

Alibakhshi, E., Ramezanzadeh, M., Bahlakeh, G., Ramezanzadeh, B., Mahdavian, M., & Motamedi, M. (2018). Glycyrrhiza glabra leaves extract as a green corrosion inhibitor for mild steel in 1 M hydrochloric acid solution: Experimental, molecular dynamics, Monte Carlo and quantum mechanics study. *Journal of Molecular Liquids*, *255*, 185–198. https://doi.org/10.1016/j.molliq.2018.01.144

Cang, H., Fei, Z., Shao, J., Shi, W., & Xu, Q. (2013). Corrosion Inhibition of Mild Steel by Aloes Extract in HCl Solution Medium. *Int. J. Electrochem. Sci.*, *8*.

Díaz, I., Cano, H., Chico, B., de la Fuente, D., & Morcillo, M. (2012). Some Clarifications Regarding Literature on Atmospheric Corrosion of Weathering Steels. *International Journal of Corrosion*, *2012*, 1–9. https://doi.org/10.1155/2012/812192

El Hamdani, N., Fdil, R., Tourabi, M., Jama, C., & Bentiss, F. (2015). Alkaloids extract of Retama monosperma (L.) Boiss. seeds used as novel eco-friendly inhibitor for carbon steel corrosion in 1 M HCl solution: Electrochemical and surface studies. *Applied Surface Science*, *357*, 1294–1305. https://doi.org/10.1016/j.apsusc.2015.09.159

El-Etre, A. Y., Abdallah, M., & El-Tantawy, Z. E. (2005). Corrosion inhibition of some metals using lawsonia extract. *Corrosion Science*, *47*(2), 385–395. https://doi.org/10.1016/j.corsci.2004.06.006

Gupta, D. K., Gurung, S., Karki, N., & Yadav, A. P. (2023). Corrosion Inhibition Performance of Euphorbia pulcherrima Bark Extract in 1M H2SO4 on Mild Steel. *NUTA Journal*, *10*(1–2), 31–44. https://doi.org/10.3126/nutaj.v10i1-2.62969

Gupta, D. K., Kafle, K. A., Das, A. K., Neupane, S., Ghimire, A., Yadav, B. D., Chaudhari, Y., Karki, N., & Yadav, A. P. (2020). Study of Jatropha Curcas Extract as a Corrosion Inhibitor in Acidic Medium on Mild Steel by Weight Loss and Potentiodynamic Methods. *Journal of Nepal Chemical Society*, *41*(1), Article 1. https://doi.org/10.3126/jncs.v41i1.30493

Gupta, D. K., Neupane, S., Singh, S., Karki, N., & Yadav, A. P. (2021). The effect of electrolytes on the coating of polyaniline on mild steel by electrochemical methods and its corrosion

behavior. *Progress in Organic Coatings*, *152*, 106127. https://doi.org/10.1016/j.porgcoat.2020.106127

Habeeb, H. J., Luaibi, H. M., Dakhil, R. M., Kadhum, A. A. H., Al-Amiery, A. A., & Gaaz, T. S. (2018). Development of new corrosion inhibitor tested on mild steel supported by electrochemical study. *Results in Physics*, *8*, 1260–1267. https://doi.org/10.1016/j.rinp.2018.02.015

Hachelef, H., Benmoussat, A., Khelifa, A., Athmani, D., & Bouchareb, D. (2016). *Study of corrosion inhibition by Electrochemical Impedance Spectroscopy method of 5083 aluminum alloy in 1M HCl solution containing propolis extract*.

Hooshmand Zaferani, S., Sharifi, M., Zaarei, D., & Shishesaz, M. R. (2013). Application of eco-friendly products as corrosion inhibitors for metals in acid pickling processes – A review. *Journal of Environmental Chemical Engineering*, *1*(4), 652–657. https://doi.org/10.1016/j.jece.2013.09.019

Hosford, W. F. (2012). *Iron and steel*. Cambridge University Press.

Hossain, N., Chowdhury, M. A., Rana, M., Hassan, M., & Islam, S. (2022). Terminalia arjuna leaves extract as green corrosion inhibitor for mild steel in HCl solution. *Results in Engineering*, *14*, 100438. https://doi.org/10.1016/j.rineng.2022.100438

Hua wenyan, Ding Li, Chen Yan, Gong bin, He Jianchang, & Xu Guili. (2007). *Determination of berberine in human plasma by liquid chromatography–electrospray ionization–mass spectrometry*. *44*.

Hussin, M. H., Jain Kassim, M., Razali, N. N., Dahon, N. H., & Nasshorudin, D. (2016). The effect of Tinospora crispa extracts as a natural mild steel corrosion inhibitor in 1M HCl solution. *Arabian Journal of Chemistry*, *9*, S616–S624. https://doi.org/10.1016/j.arabjc.2011.07.002

Kadhim A, Betti N., Al-Bahrani H. A., Al-Ghezi M.K.S., Gaaz T., Kadhum A. H., & Alamiery A. (2021). A mini review on corrosion, inhibitors and mechanism types of mild steel inhibition in an acidic environment. *International Journal of Corrosion and Scale Inhibition*, *10*(3). https://doi.org/10.17675/2305-6894-2021-10-3-2

Karki, N., Neupane, S., Chaudhary, Y., Gupta, D. K., & Yadav, A. P. (2020). *Berberis Aristata: A Highly Efficient and Thermally Stable Green Corrosion Inhibitor for Mild Steel in Acidic Medium* (7). *12*(7), Article 7.

Karki, N., Neupane, S., Chaudhary, Y., Gupta, D. K., & Yadav, A. P. (2021). Equisetum hyemale: A new candidate for green corrosion inhibitor family. *International Journal of Corrosion and Scale Inhibition*, *10*(1), Article 1. https://doi.org/10.17675/2305-6894-2021-10-1-12

Karki, N., Neupane, S., Gupta, D. K., Das, A. K., Singh, S., Koju, G. M., Chaudhary, Y., & Yadav, A. P. (2021). Berberine isolated from Mahonia nepalensis as an eco-friendly and thermally stable corrosion inhibitor for mild steel in acid medium. *Arabian Journal of Chemistry*, *14*(12), 103423. https://doi.org/10.1016/j.arabjc.2021.103423

Karthik, R., Muthukrishnan, P., Elangovan, A., Jeyaprabha, B., & Prakash, P. (2014a). Extract of *Cassia senna* as Green Inhibitor for the Corrosion of Mild Steel in 1M Hydrochloric Acid

Solution. *Advances in Civil Engineering Materials*, *3*(1), 413–433. https://doi.org/10.1520/ACEM20140010

Karthik, R., Muthukrishnan, P., Elangovan, A., Jeyaprabha, B., & Prakash, P. (2014b). Extract of *Cassia senna* as Green Inhibitor for the Corrosion of Mild Steel in 1M Hydrochloric Acid Solution. *Advances in Civil Engineering Materials*, *3*(1), 20140010. https://doi.org/10.1520/ACEM20140010

Kaya, F., Solmaz, R., & Geçibesler, İ. H. (2023a). Investigation of adsorption, corrosion inhibition, synergistic inhibition effect and stability studies of Rheum ribes leaf extract on mild steel in 1 M HCl solution. *Journal of the Taiwan Institute of Chemical Engineers*, *143*, 104712. https://doi.org/10.1016/j.jtice.2023.104712

Kaya, F., Solmaz, R., & Geçibesler, İ. H. (2023b). Investigation of adsorption, corrosion inhibition, synergistic inhibition effect and stability studies of Rheum ribes leaf extract on mild steel in 1 M HCl solution. *Journal of the Taiwan Institute of Chemical Engineers*, *143*, 104712. https://doi.org/10.1016/j.jtice.2023.104712

Koch, G. (2017). Cost of corrosion. In *Trends in Oil and Gas Corrosion Research and Technologies* (pp. 3–30). Elsevier. https://doi.org/10.1016/B978-0-08-101105-8.00001-2

Krishnegowda, P. M., Venkatesha, V. T., Krishnegowda, P. K. M., & Shivayogiraju, S. B. (2013). Acalypha torta Leaf Extract as Green Corrosion Inhibitor for Mild Steel in Hydrochloric Acid Solution. *Industrial & Engineering Chemistry Research*, *52*(2), 722–728. https://doi.org/10.1021/ie3018862

Kumari Das, A., Neupane, S., Kumar Nayak, K., Shrestha, S., Karki, N., Kumar Gupta, D., & Prasad Yadav, A. (2024). Dichloromethane -Methanol fraction of Mahonia nepalensis containing Berberine, Jatrorrhizine, and Tetrahydroberberine as corrosion inhibitor for mild steel. *Results in Chemistry*, *12*, 101866. https://doi.org/10.1016/j.rechem.2024.101866

Li, B., Wang, W., Chen, L., Zheng, X., Gong, M., Fan, J., Tang, L., Shi, Q., & Zhu, G. (2023). Corrosion inhibition effect of magnolia grandiflora leaves extract on mild steel in acid solution. *International Journal of Electrochemical Science*, *18*(4), 100082. https://doi.org/10.1016/j.ijoes.2023.100082

Li, Y., Zhao, P., Liang, Q., & Hou, B. (2005). Berberine as a natural source inhibitor for mild steel in 1M H2SO4. *Applied Surface Science*, *252*(5), 1245–1253. https://doi.org/10.1016/j.apsusc.2005.02.094

Okafor, P. C., Ebenso, E. E., El-Etre, A. Y., & Quraishi, M. A. (2012). Green Approaches to Corrosion Mitigation. *International Journal of Corrosion*, *2012*, 1–2. https://doi.org/10.1155/2012/908290

Oyekunle, D. T., Agboola, O., & Ayeni, A. O. (2019). Corrosion Inhibitors as Building Evidence for Mild Steel: A Review. *Journal of Physics: Conference Series*, *1378*(3), 032046. https://doi.org/10.1088/1742-6596/1378/3/032046

Parajuli, D., Sharma, S., Oli, H., Bohara, D., Bhattarai, D., Tiwari, A., & Yadav, A. (2022). Comparative Study of Corrosion Inhibition Efficacy of Alkaloid Extract of Artemesia

vulgaris and Solanum tuberosum in Mild Steel Samples in 1 M Sulphuric Acid. *Electrochem*, *3*(3), 416–433. https://doi.org/10.3390/electrochem3030029

Peter A. & Sharma S. K. (2017). Use of Azadirachta indica (AZI) as green corrosion inhibitor against mild steel in acidic medium: Anti-corrosive efficacy and adsorptive behaviour. *International Journal of Corrosion and Scale Inhibition*. https://doi.org/10.17675/2305-6894-2017-6-2-2

Sanaei, Z., Ramezanzadeh, M., Bahlakeh, G., & Ramezanzadeh, B. (2019). Use of Rosa canina fruit extract as a green corrosion inhibitor for mild steel in 1 M HCl solution: A complementary experimental, molecular dynamics and quantum mechanics investigation. *Journal of Industrial and Engineering Chemistry*, *69*, 18–31. https://doi.org/10.1016/j.jiec.2018.09.013

Singh, M. R. (2013). *A green Approach:A corrosion inhibition of mild steel by adhatoda vasica plant extract in 0.5 M H2SO4*.

Wang, Q., Tan, B., Bao, H., Xie, Y., Mou, Y., Li, P., Chen, D., Shi, Y., Li, X., & Yang, W. (2019). Evaluation of Ficus tikoua leaves extract as an eco-friendly corrosion inhibitor for carbon steel in HCl media. *Bioelectrochemistry*, *128*, 49–55. https://doi.org/10.1016/j.bioelechem.2019.03.001